

## Article

### Surface Plasmon Coupled Fluorescence in the Visible to Near-Infrared Spectral Regions using Thin Nickel Films: Application to Whole Blood Assays

Kadir Aslan, Yongxia Zhang, and Chris D. Geddes

*Anal. Chem.*, 2009, 81 (10), 3801-3808 • DOI: 10.1021/ac9001673 • Publication Date (Web): 08 April 2009

Downloaded from <http://pubs.acs.org> on May 15, 2009

#### More About This Article

Additional resources and features associated with this article are available within the HTML version:

- Supporting Information
- Access to high resolution figures
- Links to articles and content related to this article
- Copyright permission to reproduce figures and/or text from this article

[View the Full Text HTML](#)



ACS Publications

High quality. High impact.

Analytical Chemistry is published by the American Chemical Society. 1155 Sixteenth Street N.W., Washington, DC 20036

# Surface Plasmon Coupled Fluorescence in the Visible to Near-Infrared Spectral Regions using Thin Nickel Films: Application to Whole Blood Assays

Kadir Aslan, Yongxia Zhang, and Chris D. Geddes\*

Institute of Fluorescence, Medical Biotechnology Center, University of Maryland Biotechnology Institute, 701 East Pratt Street, Baltimore, Maryland 21202

Nickel thin films thermally evaporated onto glass supports are used to demonstrate surface plasmon coupled fluorescence (SPCF) over a broad 400 nm wavelength range (400–800 nm) for potential assays that can be run in buffer and/or whole blood. In contrast to traditional fluorescence-based assays, SPCF converts otherwise isotropic emission into highly directional and polarized emission, an attractive concept for surface assays. Theoretical Fresnel calculations performed in the ultraviolet to near-infrared spectral range (344–1240 nm) predict the near-field generation of surface plasmons in 15 and 20 nm nickel thin films. The angles of minimum reflectivity for nickel thin films with 10 nm SiO<sub>x</sub> and 30 nm polymer overcoats over the 428–827 nm wavelength range occur over a 10 degree range. To experimentally corroborate the theoretical calculations, a polymeric solution of five different fluorophores, POPC ( $\lambda_{\text{max, emission}} = 428 \text{ nm}$ ), FITC (517 nm), S101 (600 nm), Zn PhCy (710 nm), and IR 780 (814 nm), were spin coated separately onto 15 and 20 nm nickel thin films. SPCF intensity (s- and p-polarized) from fluorophores at the corresponding emission  $\lambda_{\text{max}}$  was measured at angles between 0–90 degrees. In addition, the free-space emission and SPCF intensity of FITC on 20 nm nickel thin film were also measured to demonstrate the angular-dependent nature of SPCF. SPCF from nickel thin films was p-polarized and highly directional with  $\lambda_{\text{max}}$  confirmed at an angle of 65 degrees for all the fluorophores as predicted by Fresnel calculations. The utility of nickel thin films for whole blood bioassays is demonstrated with a long-wavelength fluorophore, where the SPCF intensity of Zn PhCy (50 pM–50 μM) in whole blood at 710 nm was measured at 65 degrees. Using Fresnel calculations it is also predicted that the evanescent field above the nickel films penetrates deeper into solution than for other metals used to date for SPCF, an attractive notion in SPCF-based biosensing applications.

Surface plasmon fluorescence spectroscopy (SPFS),<sup>1</sup> a technique that utilizes the interactions of fluorescent species with thin metal films, is becoming a useful tool in the analytical biosciences. In SPFS, fluorescent species typically attached to biomolecules

are brought within close proximity to the metal surface via biorecognition events between metal surface bound biomolecules and the fluorescently labeled biomolecules as part of the bioassays constructed on the metal surface. The fluorescence emission detected from the sample side (free-space emission) or through the prism (surface plasmon coupled fluorescence, SPCF) is then used to quantify the biomolecule of interest. In this regard, attomolar sensitivity in immunoassays based on SPFS has been reported.<sup>2</sup> One can also find other reports on SPFS for DNA hybridization<sup>3–5</sup> and protein detection.<sup>6</sup>

In SPFS, two modes of excitation of the fluorescent species can be achieved: (1) Kretschmann (KR) configuration: through a prism, (2) reverse Kretschmann (RK) configuration: directly from the air or sample side.<sup>1</sup> The description of both modes of excitation has been given elsewhere.<sup>7</sup> In fluorescence-based biosensing applications that utilize an optically dense medium, such as whole blood, the KR configuration is typically considered for the excitation of fluorescent species. This is due to the effective excitation of fluorescent species by the excitation light in the form of an evanescent wave which penetrates several hundred nanometers into the optically dense medium from the surface of the metal. On the other hand, in the RK configuration, the efficiency of excitation of the fluorescent species in optically dense medium can be considerably less than as compared to KR because of the sample thickness and inner filter effect. Regardless of the excitation mode, the fluorescence emission can be detected as both free-space isotropic emission and/or highly directional SPCF emission. One can visually see the SPCF emission as a cone or as a “ring” from the back of the film when a hemispherical prism is employed.

The choice of metal in SPFS is usually gold<sup>1,8</sup> since it is inert and amenable to chemical modification without the loss of physical and electronic properties. Despite their versatility, the use of gold

- (2) Yu, F.; Persson, B.; Lofas, S.; Knoll, W. *J. Am. Chem. Soc.* **2004**, *126*, 8902–8903.
- (3) Kwon, S. H.; Hong, B. J.; Park, H. Y.; Knoll, W.; Park, J. W. *J. Colloid Interface Sci.* **2007**, *308*, 325–331.
- (4) Liu, J.; Tiefenauer, L.; Tian, S.; Nielsen, P. E.; Knoll, W. *Anal. Chem.* **2006**, *78*, 470–476.
- (5) Tawa, K.; Yao, D.; Knoll, W. *Biosens. Bioelectron.* **2005**, *21*, 322–329.
- (6) Aslan, K.; Malyn, S. N.; Geddes, C. D. *J. Immunol. Methods* **2007**, *323*, 55–64.
- (7) Aslan, K.; Previte, M. J.; Zhang, Y.; Geddes, C. D. *Anal. Chem.* **2008**, *80*, 7304–7312.
- (8) Liebermann, T.; Knoll, W.; Sluka, P.; Herrmann, R. *Colloids Surf., A* **2000**, *169*, 337–350.

\* To whom correspondence should be addressed. E-mail: geddes@umbi.umd.edu.

(1) Liebermann, T.; Knoll, W. *Colloids Surf., A* **2000**, *171*, 115–130.

thin films is limited to the visible spectral range. In recent years, there has been a resurgence in the investigation of other metals to alleviate this problem: silver<sup>9</sup> and aluminum<sup>10</sup> and zinc thin films<sup>7</sup> were shown to work in the UV and UV to visible spectral range, respectively. It was also shown that copper thin films<sup>11</sup> can also be used with fluorophores emitting >550 nm. It is important to also note that the angle of reflectivity minimum varies with the type and thickness of the metal used because of the optical properties of the metal. However, there is a continued search for metal(s) that can function in a broad wavelength range with the possibility of covering the wavelengths for many commercially available fluorophores. That is, a single metal thin film can utilize fluorophores from the UV to NIR without the need to change metal. The use of a single metal thin film for a wide range of wavelengths affords the possibility of multiplexed assays to be run on the same assay platform using multiple fluorophores (e.g., quantum dots) that can be excited with a single excitation source. Thus, bioassays can potentially be run faster at a fraction of the cost of running the same number of assays on multiple assay platforms. In addition, it would be ideal if the reflectivity minimum for such a metal thin film would occur at a fixed wavelength, which would alleviate the need to change the observation angle, as is commonly observed for silver thin films.

In this work, a detailed investigation of the utility of nickel thin films for SPCF spectroscopy is presented. Fresnel calculations were used to predict the optimum thickness of the nickel thin film and the wavelength range of light that can couple to the nickel thin films. The optimum thickness of the films was determined to be in the 15–20 nm range. The spectral regions of light that can couple to nickel thin films were calculated to be ≈344 to 1240 nm. Fresnel calculations predict the reflectivity minimum for nickel thin films to occur at a range of angles from 60–70 degrees for light at 428–827 nm. The experimental confirmation of Fresnel calculations for nickel thin films was undertaken with five different fluorophores with emission wavelengths falling in the range of 428–814 nm. The maximum value of SPCF emission intensity for all fluorophores occurred at an angle of ≈65 degrees as predicted by Fresnel calculations. From the experimental results it was concluded that 20 nm nickel thin films have potential utility in whole blood assays, which was demonstrated with a long wavelength fluorophore, Zn PhCy. Fresnel calculations were also used to predict the penetration depth of light (evanescent field), above the metal surface. It was calculated that the evanescent field penetrates to greater depth in solution than other metals used in SPFS to date, making nickel thin films an excellent choice of metal to be used in SPCF applications today.

## EXPERIMENTAL SECTION

**Materials.** All fluorophores, 1,4-bis(5-phenyl-2-oxazolyl)benzene (POPOP), fluorescein isothiocyanate (FITC), Zinc Phthalocyanine (Zn PhCy), Sulforhodamine 101(S101), IR-780 Iodide (IR780), poly(vinyl)alcohol (PVA, 98% hydrolyzed 13,000–23,000 MW), poly(methyl methacrylate) (PMMA, 100,000 MW), toluene,

- (9) Gryczynski, I.; Malicka, J.; Nowaczyk, K.; Gryczynski, Z.; Lakowicz, J. R. *J. Phys. Chem. B* **2004**, *108*, 12073–12083.
- (10) Gryczynski, I.; Malicka, J.; Gryczynski, Z.; Nowaczyk, K.; Lakowicz, J. R. *J. Anal. Chem.* **2004**, *76*, 4076–4081.
- (11) Previte, M. J. R.; Zhang, Y. X.; Aslan, K.; Geddes, C. D. *Appl. Phys. Lett.* **2007**, *91*.

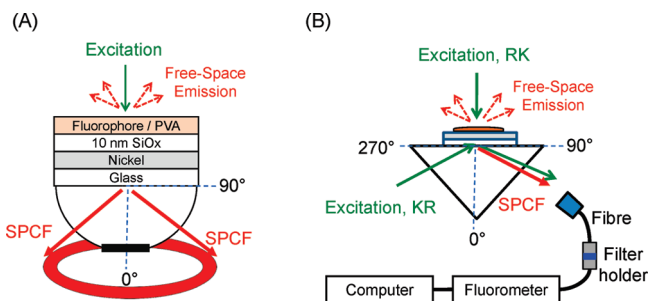


**Figure 1.** Experimental geometry. Schematic representation of experimental setup for SPCF measurements carried out with (A) a hemispherical prism is used to collect the “ring” of emission and from nickel substrates (B) a 45-degree prism that affords for Kretschmann (KR) and Reverse Kretschmann (RK) geometries to be used.

chloroform (99.8% ACS Reagent), whole blood, silicone isolator sample holders (press-to-seal), and silane-prep glass microscope slides (were purchased from Sigma-Aldrich Chemical Co. (Milwaukee, WI, U.S.A.). Nickel thin films (15 and 20 nm) with 10 nm thick SiOx overlayer were separately deposited onto silane-prep glass microscope slides by AccuCoat Inc., Rochester, NY, U.S.A.

**Methods. Sample Preparation.** The method for the deposition of fluorophores onto metallic thin films was published elsewhere.<sup>7</sup> In short, fluorophores were deposited onto nickel thin films by spin coating a solution of polymers containing the fluorophores. Stock solutions of POPOP and Zn PhCy (1 mM) were prepared in toluene and mixed with a 5% PMMA solution to make a POPOP solution with the following final concentrations: 0.1 mM POPOP and 0.1 mM Zn PhCy in 1%PMMA. Stock solutions of FITC, S101 and IR780 (1 mM in water) were then diluted with a solution of 5%PVA in water. The final concentrations of fluorophore/polymer solutions were adjusted to 0.1 mM of fluorophore and 0.1% PVA. Forty microliters of fluorophore/polymer solutions were spin-coated onto nickel thin films (1 cm × 1 cm) using a Chemat Technology Spin Coater (Model KW-4A) with the following speeds: setting 1, 9 s; setting 2, 20 s. The thickness of the polymer films was previously measured to be ≈25 nm for 0.1% PVA films, and a 1% PMMA film. It was previously shown that the thickness of the polymer film spin coated onto metal films is dependent on the size of the support, the type, and the settings of the spin coater itself.<sup>7</sup> Thus, similar solution preparation conditions and settings were used to reproduce the results presented in this study.

**Surface Plasmon Fluorescence Spectroscopy (SPFS).** Free-space and SPCF emission measurements were made according to previously published methods:<sup>7</sup> In this regard, the fluorophore-coated nickel thin films were attached to either a hemispherical or a right-angle prism made of BK7 glass with index matching fluid, cf. Figure 1. The sample was excited using either the Kretschmann (KR) or the Reverse Kretschmann (RK) configuration in SPFS measurements. A hemispherical prism was used only to collect the photographs of the SPCF “ring”. The excitation of FITC, S101, Zn PhCy, and IR780 was undertaken with a laser (473, 532, 594, and 594 nm, respectively) at an angle normal to the surface. The excitation of POPOP was from a UV light source (Mikropack D-2000 Deuterium) that was collimated to a 5 mm spot on the sample geometry at an angle normal to the surface using the RK configuration. The observations of the

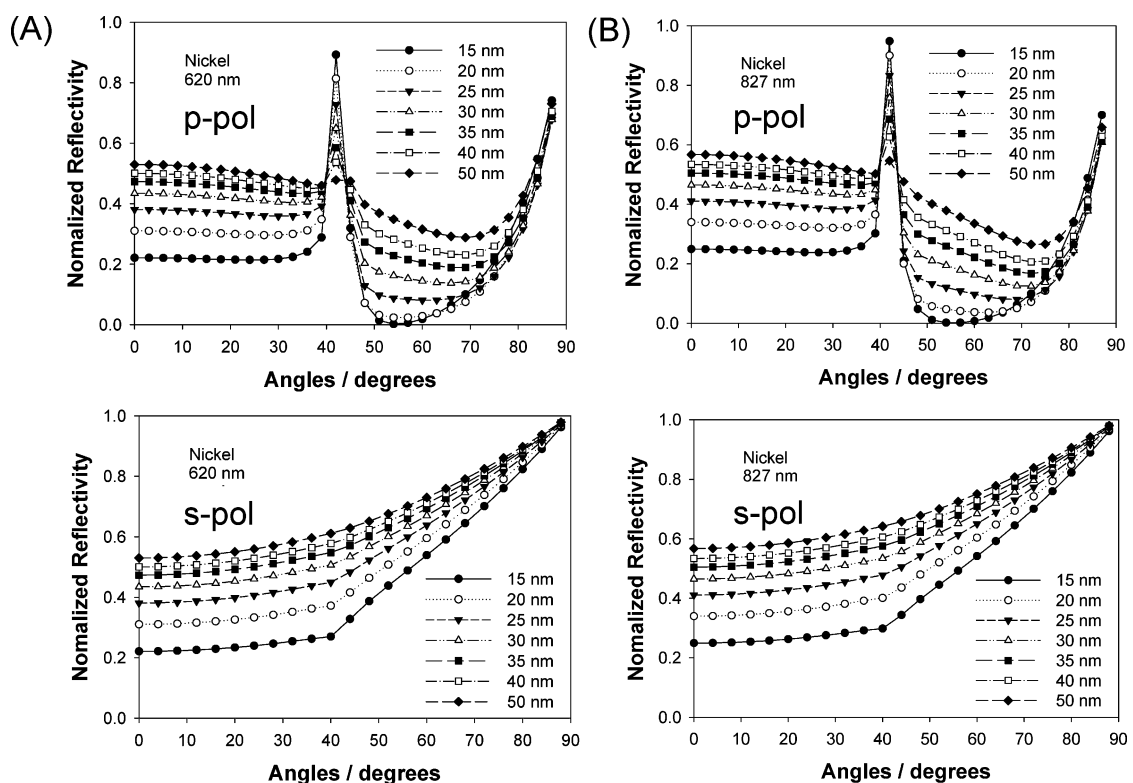


**Figure 2.** Determination of nickel substrate thickness for SPCF. Four-phase Fresnel reflectivity curves for *p*- (top) and *s*- (bottom) polarized light at (A) 620 nm and (B) 827 nm for nickel substrate thicknesses ranging from 15 to 50 nm with a 10 nm SiO<sub>x</sub> overlayer.

surface plasmon coupled and free-space emission were performed with a 600  $\mu\text{m}$  diameter fiber bundle, covered with a 200  $\mu\text{m}$  vertical slit, positioned about 15 cm from the sample. This corresponds to an acceptance angle below 0.1°. The output of the fiber was connected to an Ocean Optics HD2000+ spectrophotometer to measure the fluorescence emission spectra through a 400, 600, 700, 800 nm long-pass filters for POPOP, S101, Zn PhCy, and IR 780, respectively, and a 488 nm super notch filter (Semrock) for FITC. Real-color photographs of the SPCF emission were taken through an emission filter used for the excitation of the samples placed on a hemispherical prism.

SPCF measurements in whole blood were performed using both KR and RK configurations. In this regard, various concentrations of Zn PhCy (emission peak at 710 nm) were mixed with whole blood (1:1 v/v) and placed in two different types of commercially available sample holders attached to nickel thin films. The dimensions of the circular sample holders were (diameter  $\times$  depth): 2  $\times$  1.5 mm<sup>2</sup> or 9  $\times$  2 mm<sup>2</sup>. Total sample volume was 30 and 100  $\mu\text{L}$  for the 2  $\times$  1.5 mm<sup>2</sup> or 9  $\times$  2 mm<sup>2</sup> sample holders, respectively.

**Fresnel Calculations.** Fresnel calculations were performed according to our previously published procedure.<sup>7</sup> Penetration depth calculations were performed for metals using three-phase (glass/metal/water) Fresnel calculations. The maximum value for the *z*-component of the electric field ( $E_z^2$ ) that occurs at the angle of reflectivity minimum is normalized with respect to the highest value and plotted against the thickness (depth) above the metal.<sup>12</sup>

## RESULTS AND DISCUSSION

Figure 2 shows the results of Fresnel calculations that were employed to predict the interactions of *p*- and *s*-polarized light at 620 and 827 nm with nickel thin films with various thicknesses (15–50 nm). The reflectivity values in Figure 2 were normalized to compare the angle of minimum reflectivity for the nickel thin films of different thicknesses. It is important to note that the reflectivity minimum is indicative of the efficiency of surface plasmon generation in metals.<sup>12</sup> In SPFS, excited states (dipoles) can couple to/induce surface plasmons more effectively at the angle of reflectivity minimum, that is, coupled fluorescence quanta radiates at this angle. In addition, the extent of coupling of luminescence increases as the reflectivity value decreases. Thus, normalized reflectivity values can be semiquantitatively used to assess the utility of the thickness of thin metal films in SPFS. Figure 2A-Top and 2B-Top show that the normalized reflectivity for incident *p*-polarized light at 620 and 827 nm is minimal at 52–60 degrees for 15 nm nickel thin films. A closer look at Figure 2A-Top and 2B-Top reveals that 20 nm thick nickel films can also be used for SPCF since the normalized intensity and the angle of reflectivity minimum occur between 52–70 degrees. In addition, the extent of coupling of *s*-polarized light to surface plasmons is predicted to be the largest for 15 and 20 nm nickel thin films as shown in Figure 2, panels A-Bottom and B-Bottom. Fresnel calculations also predict that as the thickness of the nickel thin film is increased the *s*-polarized component of coupled light is decreased. Nevertheless, the extent of coupling of *p*-polarized light

(12) Knoll, W. *Annu. Rev. Phys. Chem.* 1998, 49, 569–638.

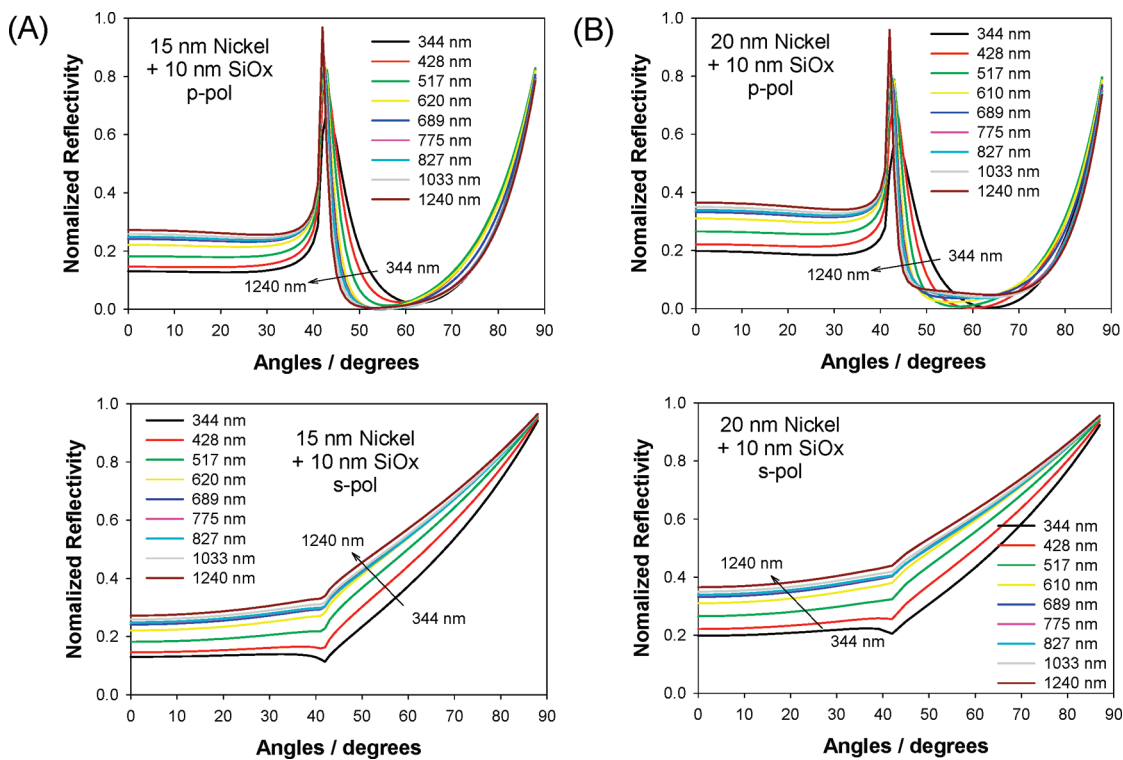


**Figure 3.** Determination of nickel substrate wavelength range for SPCF. Four-phase Fresnel reflectivity curves for *p*- (top) and *s*- (bottom) polarized light at 344, 428, 517, 620, 689, 775, 827, 1033, and 1240 nm for (A) 15 nm Ni and (B) 20 nm Ni with a 10 nm SiO<sub>x</sub> overlayer.

is predicted to be much larger than the extent of coupling of *s*-polarized light for 15 and 20 nm nickel thin films as compared to 25–50 nm nickel thin films, cf. Figure 2. In this regard, the ideal thickness for the nickel thin films for SPFS was concluded to be 15 → 20 nm. Real-color photographs of nickel thin films (Supporting Information, Figure S1) show the semi-transparent nature of these thin films.

Subsequently, the range of fluorophores that will most efficiently couple to nickel thin films was determined from four-phase Fresnel reflectivity curves that were calculated for a wide range of wavelengths (344–1240 nm) and are shown in Figure 3. As shown in Figure 3, panels A-Top and B-Top, Fresnel calculations predicted that *p*-polarized light in the wavelength range of 428–1240 nm can induce surface plasmons at a fixed range of angles (50–60 degrees and 55–65 degrees for 15 and 20 nm nickel thin films, respectively). It was also found that the angle of reflectivity minimum for 344 nm incident light is shifted to wider angles (60–70 degrees). From these calculations it can be concluded that 15 and 20 nm nickel thin films can be used in SPCF applications over the wavelength range of 344–1240 and 428–1240 nm without the need to change the observation angle, respectively. This is an *interesting prediction* which has never been reported for metal thin films for SPCF applications to date.<sup>1,7–11</sup> The extent of coupling of *s*-polarized light to nickel thin films is predicted to decrease as the wavelength of light is increased as shown in Figure 3, panels A-Bottom and B-Bottom.

It is important to emphasize the possible implications of the results shown in Figure 3. Most of the commercially available bioassays today employ fluorophores, fluorescent proteins, and quantum dots emitting at wavelengths >400 nm. Subsequently, nickel thin films are predicted to be a single assay platform in SPFS, for use in both the ultraviolet and NIR spectral range, a

much better choice than other metallic thin films. It is also interesting to place these theoretical predictions in context with the use of other metals for SPCF. In these other reports,<sup>9–11</sup> the wavelength dependence of the reflectivity minimum of the metals, allows for the angular separation of different wavelengths, at different angles. Here, nickel thin films can provide for emission at the same angle, but over a broad wavelength range, making them particularly attractive for fixed angle and fixed geometry experimental settings.

The experimental confirmation of the theoretical predictions of the Fresnel calculations was undertaken with a series of experiments, where SPCF from five different fluorophores emitting in the 428–814 nm wavelength range was measured and compared with the Fresnel calculations, which additionally account for polymer layer where fluorophores are embedded. Since both 15 and 20 nm thick nickel films were predicted to have utility in SPFS, both of these samples were used. Figure 4 shows these results for POPOP (Figure 4, panels A and B) and FITC (Figures 4, panels C and D). It is important to note that the thickness of the polymer film containing the fluorophores was kept at ≈25 nm to avoid waveguide modes that result in emission at multiple observation angles.<sup>9</sup> The maximum SPCF intensity for POPOP appears to occur at 65 degrees on both 15 and 20 nm nickel thin films as predicted by the Fresnel calculations. The SPCF intensity was significantly larger than the free-space emission (120 degrees). In addition, the extent of *p*-polarized emission was larger than the *s*-polarized emission (up to 2-fold), unlike the free-space emission where the extent of *p*- and *s*-polarized emission were somewhat similar, providing strong experimental evidence for SPCF from nickel thin films. Similar results were also observed from samples containing FITC, Figure 4, panels C and D, respectively. The maximum SPCF intensity was observed at ≈65

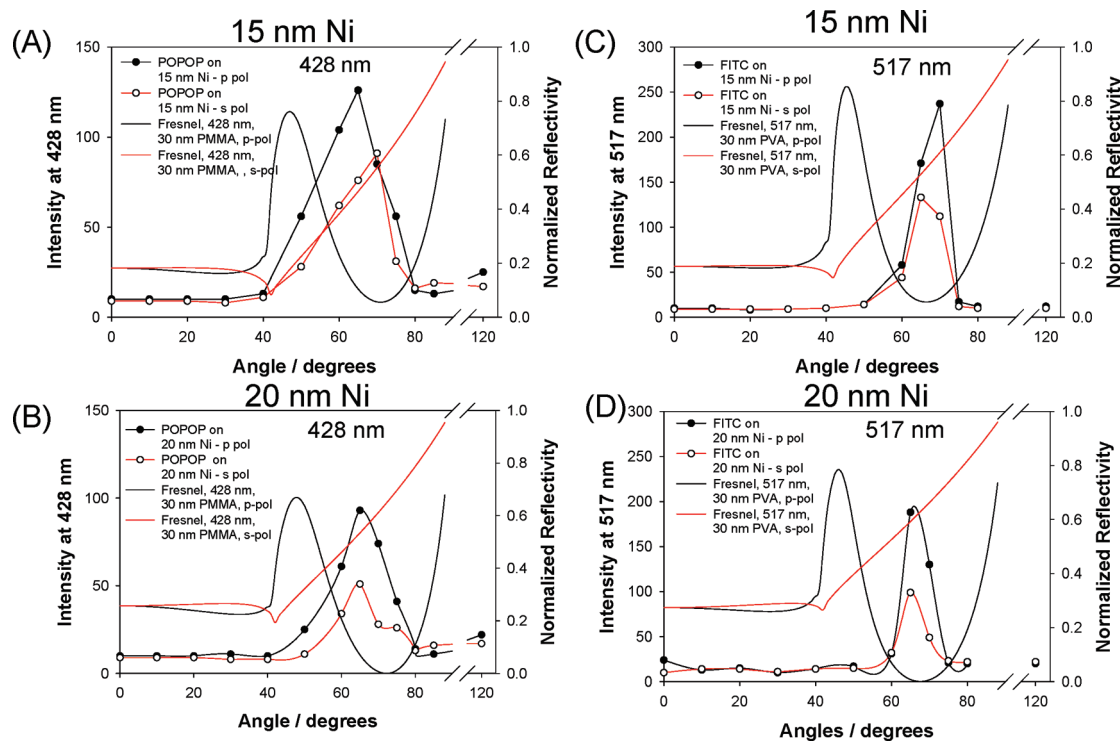


**Figure 4.** SPCF on nickel substrates from POPOP and FITC. Five-phase Fresnel reflectivity curves showing *p*- and *s*-polarized light for (A) 15 and (B) 20 nm nickel substrates with 10 nm  $\text{SiO}_x$  and 30 nm PVA overlayers. Experimental *p*- and *s*-polarized emission collected at 428 nm from 100 mL of solution (POPOP in PMMA and toluene) on nickel substrates with 10 nm  $\text{SiO}_x$ . Five-phase Fresnel reflectivity curves showing *p*- and *s*-polarized light for (C) 15 and (D) 20 nm nickel substrates with 10 nm  $\text{SiO}_x$  and 30 nm PVA overlayers. Experimental *p*- and *s*-polarized emission collected at 517 nm from 100 mL solution (FITC in PVA) on nickel substrates with a 10 nm  $\text{SiO}_x$  overlayer.

degrees, and the ratio of *p*-polarized to *s*-polarized emission was  $\approx 2$ -fold. In addition, the angular distribution of FITC emission on 20 nm nickel thin films was also measured to demonstrate the unique features (emission at a specific angle and preferential emission of *p*-polarization) of SPCF as compared to the traditionally observed isotropic free-space emission (Supporting Information, Figure S2).

The free-space emission was significantly less than the SPCF, which was due to the efficient coupled emission from fluorophores placed in close proximity to the metal. It is also important to note that the free-space emission is expected to increase as the thickness of the polymer film containing fluorophores is increased.<sup>7</sup> On the basis of the results described above, it is concluded that the performance of both 15 and 20 nm nickel thin films for SPCF from POPOP and FITC were similar.

Panels A and B of Figure 5 show that the maximum SPCF intensity at 600 nm from S101 on both 15 and 20 nm nickel thin films occurs at an observation angle of 65 degrees as predicted by Fresnel calculations. The extent of coupled *s*- and *p*-polarized emission was similar from 15 nm nickel thin films (Figure 5A), and it was larger for *p*-polarized emission from 20 nm nickel thin films (Figure 5B). This can be explained by the differences in coupling of light at 65 degrees as predicted by Fresnel calculations: for a 15 nm nickel thin film, Fresnel calculations predict that the normalized *s*-component of light to be 0.6 while the same value for a 20 nm nickel film is 0.7. That is, more *s*-polarized light is expected to couple to a 15 nm nickel thin film as compared to a 20 nm nickel thin film. Panels C and D of Figure 5 show that the maximum SPCF intensity at 710 nm for Zn PhCy is observed at 65 degrees. The extent of coupled *p*-polarized emission at 710 nm

was slightly larger than *s*-polarized emission for both 15 and 20 nm nickel thin films. In addition, the SPCF intensity for S101 and Zn PhCy was larger than the free-space emission, which is due to the placement of fluorophores within close proximity of the nickel surface.

Panels A and B of Figure 6 show the Fresnel reflectivity curves calculated for *s*- and *p*-polarized light at 814 nm and the experimental SPCF intensity values collected at 814 nm from the IR780 dye on 15 and 20 nm nickel thin films. Similar to all the fluorophores studied here, the maximum SPCF intensity from IR780 on both 15 and 20 nm nickel thin films occur at an observation angle of  $\approx 65$  degrees, which is indeed a significant benefit of our approach. These observations were consistent with the Fresnel calculations, where the reflectivity minimum was predicted to occur at  $\approx 65$  degrees. The extent of coupled *p*-polarized emission was larger than the *s*-polarized emission, up to  $\approx 2$ -fold. The results presented in Figures 5 and 6A show that nickel thin films in combination with a long wavelength fluorophore or even potentially quantum dots or fluorescent proteins have potential utility in SPCF-based whole blood assays.

The visual demonstration of SPCF from nickel thin films over a wide range of wavelengths was undertaken by capturing the “ring” of emission with a digital camera. The real-color photographs of the plasmon-coupled emission are shown in Figure 6C. In this regard, fluorophore-doped nickel thin films were placed onto a hemispherical prism, and the fluorophores were excited in the RK configuration (from the sample side at an angle normal to the nickel surface). The SPCF is emitted as a “ring” from the back of the hemispherical prism. Since SPCF intensity is signifi-

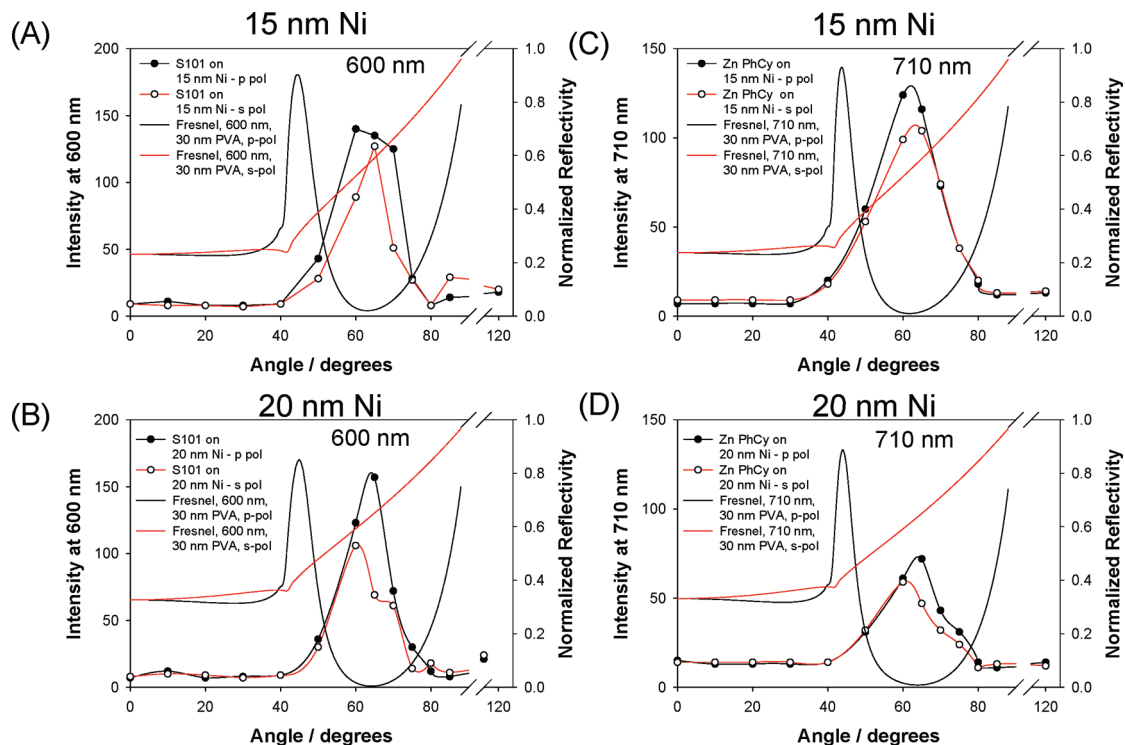


**Figure 5.** SPCF on nickel substrates from S101 and Zn PhCy. Five-phase Fresnel reflectivity curves showing *p*- and *s*-polarized light for (A) 15 and (B) 20 nm nickel substrates with 10 nm  $\text{SiO}_x$  and 30 nm PVA overlayers. Experimental *p*- and *s*-polarized emission collected at 600 nm from 100 mL solution (S101 in PVA) on nickel substrates with 10 nm  $\text{SiO}_x$ . Five-phase Fresnel reflectivity curves showing *p*- and *s*-polarized light for (C) 15 and (D) 20 nm nickel substrates with 10 nm  $\text{SiO}_x$  and 30 nm PVA overlayers. Experimental *p*- and *s*-polarized emission collected at 710 nm from 100 mL solution (Zn PhCy in toluene and chloroform) on nickel substrates with a 10 nm  $\text{SiO}_x$  overlayer.

cantly larger than the background (i.e., *p/s* contrast ratio), the image of the emission “ring” was captured with a digital camera when projected onto a screen. Figure 6C shows the emission “ring” for red (710 nm), green (517 nm) and blue (428 nm) wavelengths, demonstrating the utility of nickel thin films for SPCF applications for all three primary colors of emission.

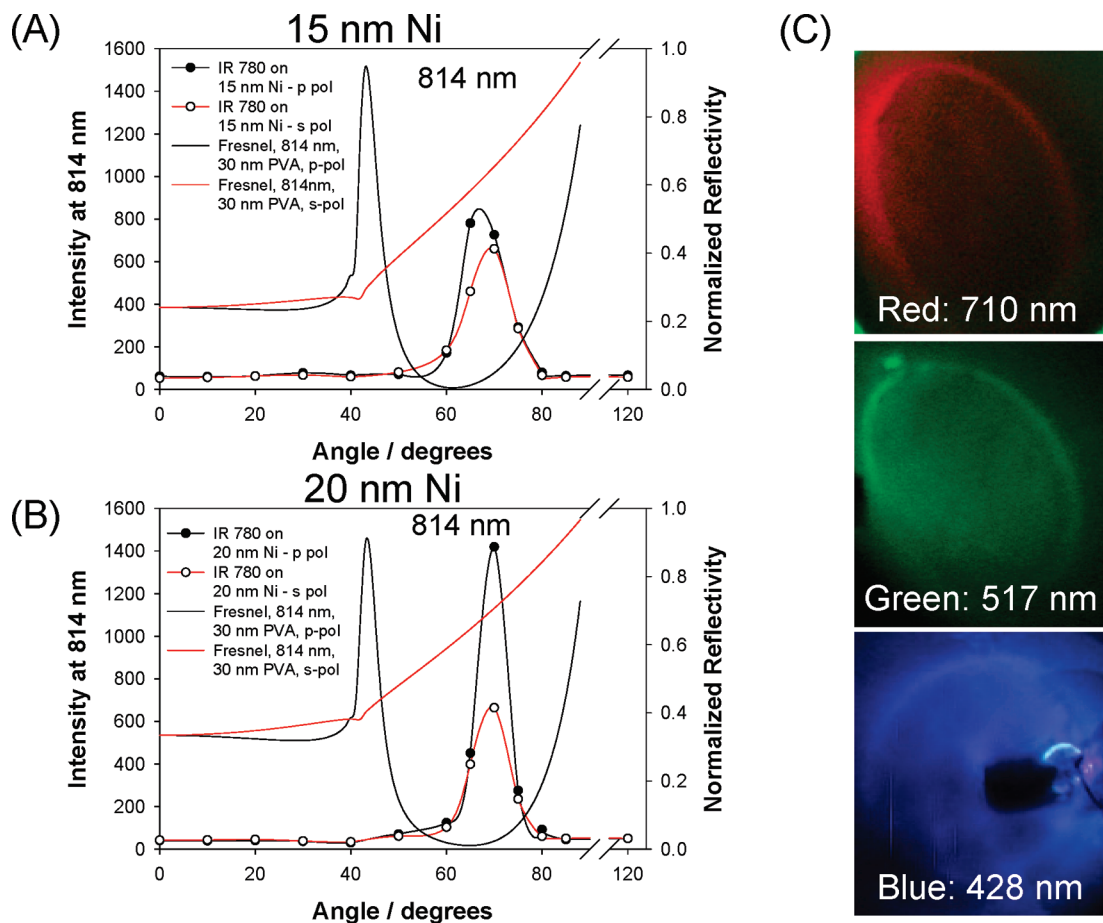
One of the interesting features of SPCF is the preferential emission of *p*-polarized light over *s*-polarized light.<sup>8,13</sup> In this regard, the theoretical values of the ratio of *p*- to *s*-polarized light (*p/s*) were calculated from normalized Fresnel reflectivity curves and compared with the *p/s* values extracted from experimental data for all fluorophores used in this study, (Supporting Information, Figure S3). Fresnel calculations predict the *p/s* values to be  $\approx 2.3$  and  $2.8$  for 15 and 20 nm nickel thin films (428–814 nm). The experimental *p/s* values appear to be similar, for the most part, to the theoretical *p/s* values for 20 nm nickel films. On the other hand, the theoretical and experimental *p/s* values only totally agree for fluorophores with emission wavelengths of 428 and 517 nm and deviate for the fluorophores with emission wavelengths  $\geq 600$  nm for 15 nm nickel films. Thus, it is concluded that 20 nm nickel thin films are the best choice for SPCF applications employing fluorophores with emission wavelengths in the visible to NIR spectral regions. It is also interesting to note that 15 nm nickel thin films can be employed for SPCF applications using fluorophores emitting in the visible spectral range. While beyond the scope of this “proof-of-concept” study, it is thought that the deviations in experimental *p/s* values from those determined

theoretically lie in the ability of our optical-trains to efficiently collect light over this broad wavelength range.

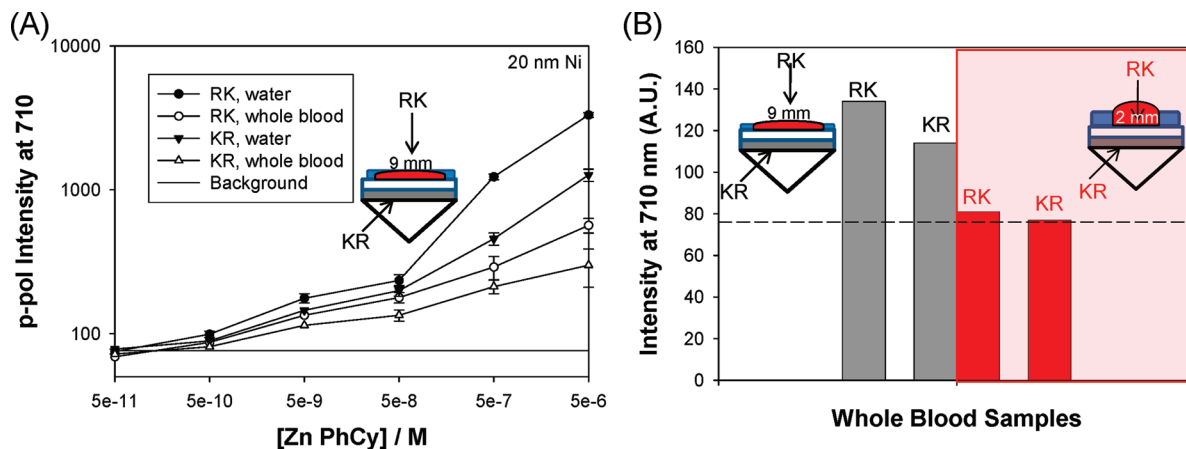
The utility of nickel thin films in SPCF-based whole blood assays was investigated using the fluorophore Zn PhCy (emission peak at 710 nm) and 20 nm nickel thin films. In this regard, a solution of Zn PhCy at various concentrations was mixed with whole blood and placed in a sample holder that is attached to nickel thin films. Since whole blood is an optically dense medium, two different sample holders (Diameter  $\times$  Depth) =  $9 \times 2 \text{ mm}^2$  and  $2 \times 1.5 \text{ mm}$  were employed to investigate the effect of sample volume on the measured SPCF intensity. Total sample volume (including whole blood and a solution of fluorophores) was 30 and 100  $\mu\text{L}$  for  $2 \times 1.5 \text{ mm}^2$  and  $9 \times 2 \text{ mm}^2$  sample holders, respectively. In addition, two configurations for excitation, KR and RK configurations were also used. In the RK configuration, the fluorophores are excited from the sample side normal to the surface, and the excitation of fluorophores is through the prism placed under the nickel thin films in the KR configuration as shown in Figures 1B and 7A-Inset.

Figure 7A shows the SPCF intensity at 710 nm for the various concentrations of Zn PhCy mixed with whole blood (in the diameter  $\times$  depth =  $9 \times 2 \text{ mm}^2$  sample holder) using KR and RK configurations. In additional experiments, whole blood was replaced by water to simulate SPCF-based bioassays run in buffer using both KR and RK configurations. As expected, the SPCF intensity from fluorophores mixed with whole blood was lower than for fluorophores in water. Larger SPCF intensities were measured from all samples in the RK configuration. It is important to note that the diameter of the sample holder (9 mm) allowed the mixture of fluorophores in whole blood to

(13) Knoll, W.; Zizlsperger, M.; Liebermann, T.; Arnold, S.; Badia, A.; Liley, M.; Piscevic, D.; Schmitt, F. J.; Spinke, J. *Colloids Surf, A* **2000**, *161*, 115–137.



**Figure 6.** SPCF on nickel substrates from IR 780. Five-phase Fresnel reflectivity curves showing *p*- and *s*- polarized light for (A) 15 and (B) 20 nm nickel substrates with 10 nm  $\text{SiO}_x$  and 30 nm PVA overlayers. Experimental *p*- and *s*- polarized emission collected at 814 nm from 100 mL solution (IR 780 in PVA) on nickel substrates with 10 nm  $\text{SiO}_x$  overlayer. (C) Real-color photographs of red (710 nm), green (517 nm), and blue (428 nm) SPCF emission from samples placed on a hemispherical prism. An excitation filter corresponding to the wavelength of excitation was placed in front of the digital camera.



**Figure 7.** Whole blood measurements. (A) SPCF measurements in whole blood using Kretschmann (KR) and Reverse Kretschmann (RK) geometries. (B) Investigation of the effect of sample (containing whole blood) volume and thickness on the SPCF intensity. The solution of fluorophore was omitted in the sample labeled "background".

spread throughout the sample holder affording for the excitation of fluorophores and thus the detection of SPCF emission. It is also important to note that although the dynamic range of emission intensity is 10-fold lower in whole blood samples as compared to water samples, the background emission is still significantly lower than the intensity values in whole blood

samples, and thus it is concluded that SPCF can be used in real life whole blood assays.

In addition, the effect of the volume and the shape of sample holder on the SPCF intensity were investigated using another commercially available sample holder (diameter  $\times$  depth = 2  $\times$  1.5 mm<sup>2</sup>, 30  $\mu\text{L}$  sample volume) and compared with the results

obtained using the larger sample holder ( $100\ \mu\text{L}$ ). Figure 7B shows the comparison of SPCF intensity collected from a mixture of  $50\text{ nM}$  Zn PhCy mixed with whole blood in both sample holders. The use of the smaller sample holder resulted in SPCF intensities very close to background levels, in comparison to detectable SPCF intensities from the larger sampler holder using both KR and RK configuration. In the smaller sample holder the mixture of fluorophore solution and whole blood prevented the appropriate excitation of fluorophores to yield any detectable signal. This can be explained by the increase in the path length of light through whole blood.

It is well-known that light incident upon a metallic thin film can propagate as an evanescent wave along the metal thin film/dielectric interface ( $x$ -direction).<sup>12</sup> In addition, the evanescent wave has an amplitude perpendicular to the metal thin film/dielectric interface and decays exponentially in the  $z$ -direction.<sup>12</sup> The penetration depth of this light into the dielectric is in the order of several hundred nanometers and indeed provides for the opportunity for the selective excitation of fluorophores in close-proximity to the metal thin film. The comparison for the calculated penetration depths (using Fresnel calculations) for light at  $620\text{ nm}$  above nickel, silver, copper, and gold thin films were also made (Supporting Information, Figure S4). Fresnel calculations predict that at a distance of  $500\text{ nm}$  above nickel thin films, the evanescent field at  $620\text{ nm}$  wavelength can retain  $40\%$  of its original intensity as compared to  $1\%$  of light that can penetrate to that distance for other metal films used in SPCF. This prediction makes nickel thin films highly attractive in SPCF-based bioassays as compared to gold, silver, zinc, and aluminum given the following:

(1) That more light can be potentially detected from fluorescent species present above nickel thin films, which is especially attractive for cell-based assays. Given that the size of cells and other microorganisms are  $\geq 1\ \mu\text{m}$ , the collection of more light in these assays will potentially lower the detection limit of the assays.

(2) A wide variety of biological assays (immunoassays (e.g., cardiac markers,<sup>14</sup> IgG) DNA hybridization (hepatitis C<sup>15</sup>), ELISAs) can be constructed on nickel thin films, and have comparable if not better sensitivity to gold and silver, within the same penetration depths.

(3) Nickel is an inexpensive metal to prepare surfaces for SPCF applications, as compared to gold and silver.

- 
- (14) Matveeva, E.; Gryczynski, Z.; Gryczynski, I.; Malicka, J.; Lakowicz, J. R. *Anal. Chem.* **2004**, *76*, 6287–6292.  
(15) Aslan, K.; Previte, M. J.; Zhang, Y.; Geddes, C. D. *J. Immunol. Methods* **2008**, *331*, 103–113.  
(16) Schmid, M.; Zimmermann, S.; Krug, H. F.; Sures, B. *Environ. Int.* **2007**, *33*, 385–390.

(4) While the toxicity of nickel is of great interest at the cellular level,<sup>16</sup> protective  $\text{SiO}_2$  layers can readily be incorporated to prevent the direct contact of both cells and/or users to nickel. Interestingly, polymer coatings can also be used, where the effect of the both the polymer thickness and nature of the material can be modeled using Fresnel calculations.

(5) Fresnel calculations show broad wavelength transmission, suggesting applicability to analytical sensing in the ultraviolet to NIR spectral regions.

(6) Both our theoretical calculations and experimental findings show that coupled luminescence through thin Nickel films occurs over a narrow range of angles. This suggests that “fixed angle” geometries can be used over a broad range of wavelength applications, as compared to silver and gold films,<sup>6,9</sup> where there is a strong dependence of emission angle with coupling wavelength.

## CONCLUSIONS

The use of nickel thin films in SPFS to generate highly polarized and directional emission is demonstrated. Fresnel calculations predict that light at  $344\text{--}1240\text{ nm}$  can effectively couple to  $15$  and  $20\text{ nm}$  nickel thin films at a fixed  $10$  degree wide observation angle, located between  $60$  and  $70$  degrees from the normal of the surface. SPCF from five different fluorophores with emission wavelengths falling in the range of  $428\text{--}814\text{ nm}$  were experimentally observed at an angle of  $\approx 65$  degrees, in excellent agreement with Fresnel calculations. It was found that the extent of measured *p*-polarized light was larger than (up to  $\approx 2.8$  fold) that of *s*-polarized light, confirming the observed emission from the back of the nickel film is indeed nickel plasmon-coupled. From the experimental results it was concluded that  $20\text{ nm}$  nickel thin films have potential utility in whole blood assays, which was demonstrated with a near-IR fluorescent probe Zn PhCy (emission peak at  $710\text{ nm}$ ). Fresnel calculations also predict that light can penetrate to a greater distance than other metal thin films, making the nickel thin films an excellent choice of metal to be used in SPCF applications today.

## ACKNOWLEDGMENT

The authors would like to acknowledge UMBI, MBC, and the IoF for salary support.

## SUPPORTING INFORMATION AVAILABLE

Additional information as noted in the text. This material is available free of charge via the Internet at <http://pubs.acs.org>.

Received for review January 22, 2009. Accepted March 27, 2009.

AC9001673